EAST EUROPEAN JOURNAL OF PHYSICS. 1. 284-289 (2025)
DOI:10.26565/2312-4334-2025-1-33 ISSN 2312-4334

COMPARATIVE STUDY AND ANALYTICAL MODELING OF AlGaN/GaN HEMT AND MOSHEMT BASED BIOSENSORS FOR BIOMOLECULES DETECTION

Abdellah Bouguenna[a]*, Abdelhadi Feddag[b], Driss Bouguenna[c,d], Ibrahim Farouk Bouguenna[e]
[a]*Electrical Engineering Laboratory of Oran, Electronics Department, Electrical Engineering Faculty, Sciences & Technology University of Oran (MB-USTO), 31000, Oran, Algeria*
[b]*Department of Electronics. Faculty of Electrical Engineering University of Sciences and Technology of Oran, Microsystems and Embedded Systems Laboratory of Oran, Algeria*
[c]*Geomatics, Ecology and Environment Laboratory, Nature and Life Science Faculty, Mustapha Stambouli University of Mascara, 29000, Mascara, Algeria*
[d]*Common Core Science and Technology Department, Sciences and Technology Faculty, Mustapha Stambouli University of Mascara, 29000, Mascara, Algeria*
[e]*Electrical Engineering Department, Sciences and Technology Faculty, Mustapha Stambouli University of Mascara, Mascara 29000, Algeria*
**Corresponding Author e-mail: abdellah.bouguenna@univ-usto.dz*
Received December 19, 2024; revised January 22, 2025; accepted January 25, 2025

In this study, a model has been developed to analyze AlGaN/GaN high-electron-transistor (HEMT) and metal-oxide semiconductor high-electron-transistor (MOSHEMT) based biosensors. The model focuses on detecting biomolecules such as ChOx, protein, streptavidin and uricase by modulating the dielectric constant. The sensitivity parameters used for biomolecule detection include drain current, transconductance, and drain off sensitivity. The dielectric constant is adjusted based on the specific biomolecule being sensed by the biosensor. The variation in dielectric leads to changes in drain current, with an increase or decrease depending on the positive charge of the biomolecules. The HEMT device exhibits greater variations in drain current, transconductance, and drain off sensitivity compared to the MOSHEMT device when the biomolecule is present in the cavity region. The simulation results are validated by comparing them with Atlas-TCAD (atlas-technology computer aided design) and experimental data, showing excellent agreement.
Keywords: *AlGaN/GaN; HEMT; MOSHEMT; Biosensors; Biomolecules*
PACS: 87.85.fk

1. INTRODUCTION

For the detection of biochemical compounds such as enzymes, biological molecules, antibodies, etc the biosensors use chemical reactions [1]. GaN-based devices are good compared to silicon-based devices due to their large bandgap (3.4 eV), large electron saturation velocity (2.5×10^7 cm/s), and high operating temperature [2, 3]. AlGaN/GaN HEMT structures are widely utilized in biosensors due to their remarkable biocompatibility, stable material characteristics, and remarkable sensitivity to surface charge. This is primarily assigned to the close proximity of the two-dimensional electron gas (2DEG) channel to the surface, which typically reaches a density of approximately 10^{13} cm^{-2}. [4, 5]. The 2DEG are generated by spontaneous and piezoelectric polarization that are moderated by positive charges at the surface [6]. An oxide layer such as Al_2O_3 [7], is entered between barrier and gate metal which results HEMTs becomes MOSHEMTs [5, 8, 9]. The AlGaN barrier layer readily binds specific biomolecules, leading to variations in surface charges at the AlGaN/GaN interface [1]. Extensive research has been undertaken on AlGaN/GaN HEMT for the detection of various biomolecules, including proteins [10], Hg^{2+} [11], DNA [12], PSA [13], and c-erbB^{-2} [14]. This paper offers a comparative study between AlGaN/GaN HEMT and MOSHEMT based biosensors, focusing on the introduction of biomolecules into a nanogap cavity. The comparison aims to evaluate the impact of oxide material on the performance of these biosensors. To assess their suitability for biosensing applications, we simulated the I_{ds}-V_{gs}, I_{ds}-V_{ds}, transconductance, and sensitivity parameters for different biomolecules detection.

2. STRUCTURES OF AlGaN/GaN HEMT& MOSHEMT DEVICES

The diagram in Fig. 1 illustrates the structure of AlGaN/GaN HEMT and MOSHEMT devices. In the case of HEMT, the layers are grown in the following order: metal/AlGaN/GaN. In the MOSHEMT case. Additionally, a GaN buffer layer is grown on an Al_2O_3 substrate.

Figure 1. Model of AlGaN/GaN biosensors. *(a)* HEMT and *(b)* MOSHEMT

Cite as: A. Bouguenna, A. Feddag, D. Bouguenna, I.F. Bouguenna, East Eur. J. Phys. 1, 284 (2025), https://doi.org/10.26565/2312-4334-2025-1-33

3. ANALYTICAL MODEL OF DEVICES

In this paper, the analytical model taken from paper [15].
The analytical expression of the drain current can be formulated as

$$I_d = \frac{W_g \mu_0 C_{eff}}{L_g \delta} \left\{ \sum_{i=0}^{6} k_i \left(\psi_{gd}^i - \psi_{gs}^i \right) + k_0 ln \frac{\psi_{gd}}{\psi_{gs}} \right\} \quad (1)$$

where μ_0 is low field mobility. W_g and L_g are the width and the length of gate, respectively. $\psi_{gs} = \left(V_{gs} - V_{th} - V_s\right)^{1/3} + 2\theta$, $\psi_{gd} = \left(V_{gs} - V_{th} - V_{ds}\right)^{1/3} + 2\theta$, $\delta = V_d - V_s / E_T L_g$, $\theta = \lambda/3\,(C_{eff}/q)^{2/3}$ and E_T is the critical field.

The transconductance (g_m) is the derivation of the drain current by gate voltage at $V_{ds} = const$, it can be defined as

$$g_m = \left. \frac{\partial I_{ds}}{\partial V_{gs}} \right|_{V_{ds}=const}. \quad (2)$$

The transconductance can be extracted from Eq. (1)

$$g_m = \frac{\mu_0 W_g C_{eff}}{\rho L_g} \left[\frac{1}{3(\psi_{gd} - 2\theta)^2 - 3(\psi_{gs} - 2\theta)^2} \right] \Omega_1. \quad (3)$$

Where

$$\Omega_1 = \begin{bmatrix} \frac{288\theta^6}{(\psi_{gd} - \psi_{gs})} + 272\theta^5 + 1920\theta^4 (\psi_{gd} - \psi_{gs}) + 600\theta^3 (\psi_{gd} - \psi_{gs})^2 \\ -280\theta^2 (\psi_{gd} - \psi_{gs})^3 + 195\theta (\psi_{gd} - \psi_{gs})^4 - 18 (\psi_{gd} - \psi_{gs})^5 \end{bmatrix}. \quad (4)$$

4. RESULTS AND DISCUSSION

We will discuss the comparison of AlGaN/GaN HEMT and MOSHEMT based biosensors. The material parameters and their corresponding values employed for the simulation are outlined in Table 1 and Table 2. Furthermore, the biomolecule permittivity used in this study is listed in Table 3, and the specific values for the two different device types are delineated in Table 4.

Table 1. Constants terms. [16]

Constants	Expressions
k_0	$-288\theta^6$
k_1	$272\theta^5$
k_2	$-960\theta^4$
k_3	$200\theta^3$
k_4	$-70\theta^2$
k_5	$39\,\theta$
k_6	-3

Table 2. Parameters used in numerical simulations

Parameters	Quantities	Values	Units	Refs.
E_T	Critical electric field	178×10^5	V/m	[3]
φ_M	Metal work function	4.5	eV	[3]
φ_0	Natural level Potential	1.2	eV	[3]
μ_0	Low field mobility	0.06	m^2/Vs	[3]
N_D	Doping concentration	1.5×10^{16}	m^{-3}	[3]
γ_0	Experimental parameter	4.12×10^{-12}	$Vcm^{4/3}$	[17]

Table 3. Dielectric constants of biomolecules [18, 19]

Biomolecules	Dielectric constants
ChOx	3.3
Protein	2.5
Streptavidin	2.1
Uricase	1.54

Table 4. Device parameters used in simulation

Parameters	Description	Fig. 2a [20] Sample 1	Fig. 2b [21] Sample 2	Fig. 4, 5 and 6 Our model
x (%)	Al mole fraction	15	20	30
$\varepsilon_{ox}(F/m^2)$	Oxide permittivity	-	9.1 ε_0	9.1 ε_0

Parameters	Description	Fig. 2a [20] Sample 1	Fig. 2b [21] Sample 2	Fig. 4, 5 and 6 Our model
σ_{pol} (m^{-2})	Spontaneous polarization charge	1.15×10^{17} [22]	1.7×10^{17} [22]	1.55×10^{17} [22]
$d_{AlGaN}(nm)$	Barrier thickness	22	30	15
$L_g(\mu m)$	Gate length	1	1	0.3
$W_g(\mu m)$	Gate width	75	100	100
t_{ox} (nm)	Oxide thickness	-	16	10
h_{cavity} (nm)	Cavity width	-	-	10

The output characteristics of the AlGaN/GaN HEMT and MOSHEMT devices are compared in Fig. 2(a) and Fig. 2(b), respectively. The results from our model show a strong agreement with the experimental data [20] and [21]. Besides, the dimensions of the devices used in the experimental data were replicated exactly to validate our results. Furthermore, Matlab calculations and Atlas-TCAD were used to simulate the devices for sample 1 and sample 2, as shown in Fig. 2.

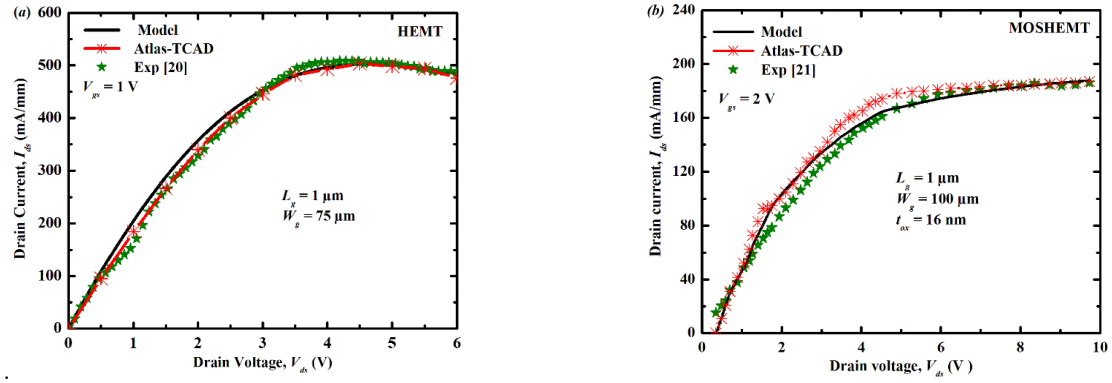

Figure 2. *I-V* output characteristics of GaN HEMT and MOSHEMT devices.
(a) HEMT and *(b)* MOSHEMT with experimental data [20] and [21], respectively

Fig. 3 illustrates the transfer characteristics of the devices with and without biomolecules. When the biomolecule is present in the cavity region, a variation in the drain current is observed. This change in drain current can be considered as a sensing parameter for biomolecule detection. Specifically, at a drain voltage of 5 V, the change in drain current is superior in HEMT device compared to MOSHEMT device. For uricase, streptavidin, protein, and ChOx, the variation in drain current is (35.69, 64.45, 81.3, and 108.36) mA in AlGaN/GaN HEMT, respectively. In contrast, the change in drain current is (7.93, 15.2, 19.88, and 28.18) mA in AlGaN/GaN MOSHEMT, respectively.

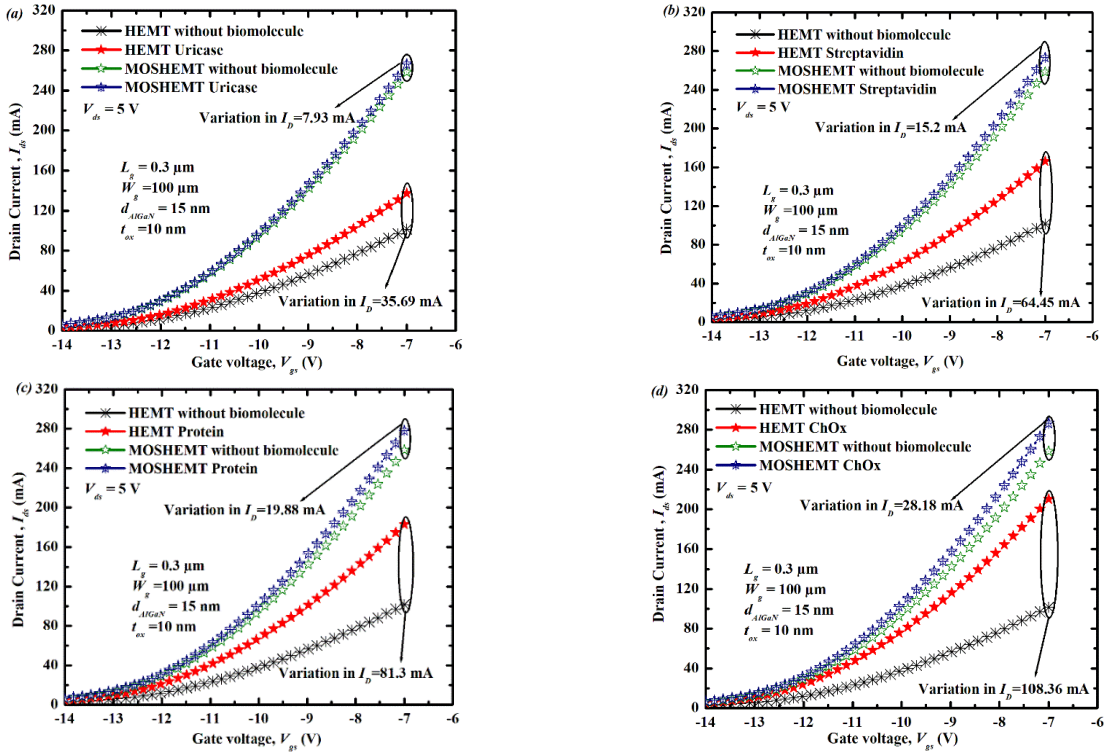

Figure 3. *I–V* transfer characteristics with different biomolecules of the both biosensors.
Change of drain current for *(a)* uricase, *(b)* streptavidin, *(c)* protein and *(d)* ChOx, respectively

Furthermore, the transconductance characteristics of HEMT and MOSHEMT devices with different biomolecules are presented in Figs. 4(a) and 4(b). The introduction of biomolecules into the cavity region leads to a change in the threshold voltage (V_{th}) and subsequently affects the transconductance (g_m). This change in transconductance can serve as a reliable sensing parameter. Notably, the HEMT devices demonstrate a greater variation in transconductance compared to the MOSHEMT devices, as shown in Figs. 4(a) and 4(b). Specifically, the variation in transconductance is (21.58, 20.05, 54.51, and 76.98) mS/mm for uricase, streptavidin, protein, and ChOx in the case of HEMT, respectively. Conversely, the variation in transconductance is (8.19, 15.86, 20.89, and 29.99) mS/mm for uricase, streptavidin, protein, and ChOx in the case of MOSHEMT, respectively.

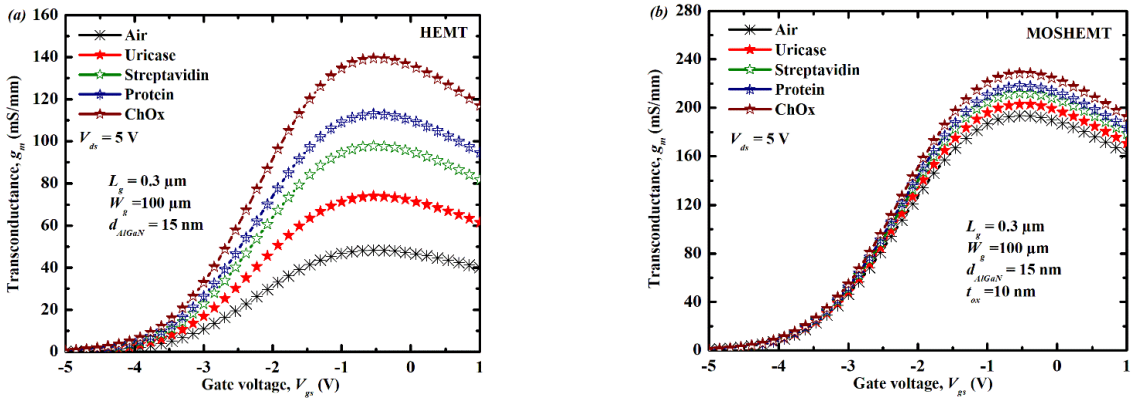

Figure 4. Comparison of the modeled transconductance characteristics with different biomolecules *(a)* HEMT and *(b)* MOSHEMT based biosensors

In Fig. 5, the sensitivity parameter of HEMT and MOSHEMT devices is compared. The results clearly indicate that the sensitivity parameter (S_{Ioff}) is significantly greater in the HEMT device compared to the MOSHEMT device. Among all the biomolecules tested, the ChOx biomolecule exhibits the highest sensitivity for the HEMT device.

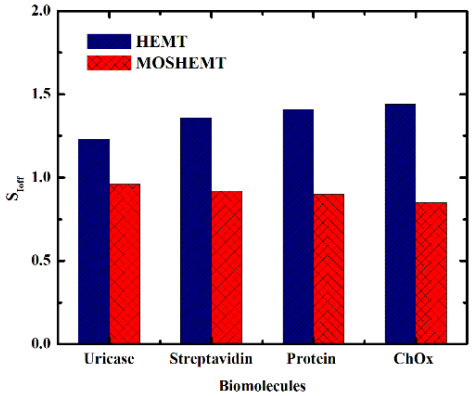

Figure 5. Sensitivity for AlGaN/GaN HEMT and MOSHEMT biosensors

Fig. 6 depicts an escalation in the relative change (sensitivity of drain current). The relative change in drain current is defined as $\Delta_{Ids} = I_{ON}^{Air} - I_{ON}^{Bio}$ [23]. The minimum and maximum relative change observed is (139.07 and 260.8) mA for uricase and ChOx for HEMT and (26.57 and 115.03) mA for uricase and ChOx for MOSHEMT, respectively.

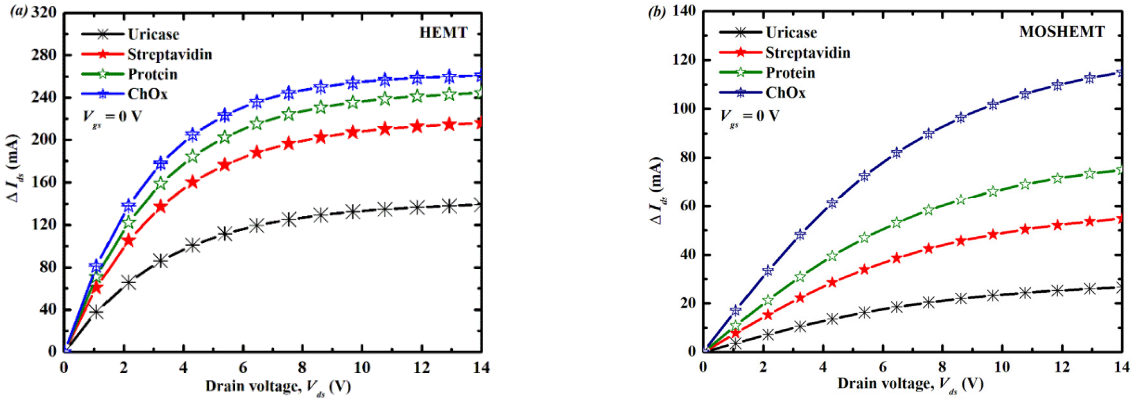

Figure 6. Relative drain ON current sensitivity for *(a)* HEMT and *(b)* MOSHEMT

Table 5. Comparative extracted values of AlGaN/GaN HEMT and MOSHEMT based biosensors.

Biomolecules	Change in drain current ΔI_D (mA)		Drain-off sensitivity (S_{Ioff})	
	AlGaN/GaN HEMT	AlGaN/GaN MOSHEMT	AlGaN/GaN HEMT	AlGaN/GaN MOSHEMT
Uricase	35.69	7.93	1.23	0.96
Streptavidin	64.45	15.2	1.36	0.92
Protein	81.3	19.88	1.41	0.9
ChOx	108.36	28.18	1.44	0.85

CONCLUSION

The analytical modeling of the both devices was proposed and compared between each other. There is a variation in drain current density and higher transconductance when the cavity region is occupied with biomolecules. This suggests that the GaN-based HEMT and MOSHEMT biosensors perform well for biosensing applications. The results obtained indicate that AlGaN/GaN HEMT based biosensors have been presented a greater change in drain current (ΔI_{on}) and sensitivity for various biomolecules. The saturation drain current and 2DEG concentration increase as the distance between the sensing area and 2DEG channel increases. However, the modulation ability of surface charge on device performance decreases with the increased sensing area-to-channel distance [24]. This implies that the sensing sensitivity decreases in AlGaN/GaN MOSHEMT based biosensors.

Conflict of interest: The authors state no conflict of interest.

ORCID

Abdellah Bouguenna, https://orcid.org/0000-0003-3492-5418; **Abdelhadi Feddag**, https://orcid.org/0009-0004-3817-0539
Driss Bouguenna, https://orcid.org/0000-0002-0660-9576; **Ibrahim Farouk Bouguenna**, https://orcid.org/0000-0001-8631-8172

REFERENCES

[1] H.M. Shaveta, A. Maali, and C. Rishu, "Rapid detection of biomolecules in a dielectric modulated GaN MOSHEMT," J. Mater. Sci: Mater Electron, **31**, 16609–16615 (2020). https://doi.org/10.1007/s10854-020-04216-7
[2] S. Verma, S.A. Loan, and A.G. Alharbi, "Polarization engineered enhancement Mode GaN HEMT: Design and Investigation," Superlattices Microstruct. **119**, 181–193 (2018). https://doi.org/10.1016/j.spmi.2018.04.041
[3] S.A. Loan, S. Verma, and A.R.M. Alamoud, "High performance charge plasma based normally-Off GaN MOSFET," IET Electron. Lett. **52**(8), 656–658 (2016). https://doi.org/10.1049/el.2015.4517
[4] Z. Gu, J. Wang, B. Miao, L. Zhao, X. Liu, D. Wu, and J. Li, "Highly sensitive AlGaN/GaN HEMT biosensors using an ethanolamine modification strategy for bioassay applications," RSC Advance, **9**, 15341–15349 (2019). https://doi.org/10.1039/C9RA02055A
[5] S.N. Mishra, R. Saha, and K. Jena, "Normally-Off AlGaN/GaN MOSHEMT as lebel free biosensor," ECS J. Solid State Sci. Technol. **9**, 1–15 (2020). https://doi.org/10.1149/2162- 8777/aba1cd
[6] S.J. Pearton, B.S. Kang, Kim S. Kim, F. Ren, B.P. Gila, C.R. Abernathy, *et al*., "GaN-based diodes and transistors for chemical, gas, biological and pressure sensing," J. Phys: Condens. Matter, **16**, R961–R994 (2004). https://doi.org/10.1088/0953-8984/16/29/R02/meta
[7] A. Varghese, C. Periasamy, and L. Bhargava, "Fabrication and charge deduction-based sensitivity analysis of GaN MOS-HEMT device for glucose, MIG, C-erbB-2, KIM-1 and PSA detection," IEEE Trans. Nanotechnol. **18**, 747–755 (2019). https://doi.org/10.1109/TNANO.2019.2928308
[8] A. Koudymov, H. Fatima, G. Simin, J. Yang, M.A. Khan, A. Tarakji, X. Hu, *et al*., "Maximum current in nitride-based heterostructure Field-Effect Transistors," Appl. Phys. Lett, **80**, 3216–3218 (2002). https://doi.org//10.1063/1.1476054
[9] M.A. Khan, X. Hu, G. Sumin, A. Lunev, J. Yang, R. Gaska, and M.S. Shur, "AlGaN/GaN Metal Oxide Semiconductor Heterostructure Field Effect Transistor," IEEE Elec. Dev. Letters, **21**, 63–65 (2000). https://doi.org//10.1109/55.821668
[10] C.C. Huang, G.Y. Lee, J.I. Chyi, H.T Cheng, C.P Hsu, Y.R Hsu, C.H. Hsu, *et al*., **"**AlGaN/GaN high electron mobility transistors for protein–peptide binding affinity study," Biosens. Bioelectron. **41**, 717–722 (2012). https://doi.org/10.1016/j.bios.2012.09.066
[11] J. Cheng, J. Li, B. Miao, J. Wang, Z. Wu, D. Wu, and R. Pei, "Ultrasensitive detection of Hg^{2+} using oligo nucleotide functionalized AlGaN/GaN High Electron Mobility Transistor," Appl. Phys. Lett, **105**, 083121-1–083121-4 (2014). https://doi.org//abs/10.1063/1.4894277
[12] S.U. Schwarz, S. Linkohr, P. Lorenz, S. Krischok, T. Nakamura, V. Cimalla, C.E. Nebel, and O. Ambacher, "DNA-sensor based on AlGaN/GaN High Electron Mobility Transistor," Phys. Status Solidi A, **208**, 1626–1629 (2011). https://doi.org/10.1002/pssa.201001041
[13] B.S. Kang, H.T. Wang, T.P. Lele, Y. Tseng, F. Ren, S.J. Pearton, J.W. Johnson, *et al*., "Prostate specific antigen detection using high electron mobility transistors," Appl. Phys. Lett. **91**, 112106 (2007). https://doi.org/10.1063/1.2772192
[14] K.H. Chen, B.S. Kang, H.T. Wang, T.P. Lele, F. Ren, Y.L. Wang, C.Y. Chang, *et al*., "C-erbB-2 sensing using AlGaN/GaN High Electron Mobility Transistors for breast cancer detection," Appl. Phys. Lett. **92**, 192103-1–192103-3 (2008), https://doi.org/abs/10.1063/1.2926656
[15] A. Bouguenna, D. Bouguenna, A.B. Stambouli, and S.A. Loan, "Comparative Study and Modeling of AlGaN/GaN Heterostructure HEMT and MOSHEMT Biosensors," Ijneam, **16**(3), 511–522 (2023). https://doi.org/10.58915/ijneam.v16i3.1268
[16] K. Jena, R. Swain, and T.R. Lenka, "Effect of thin gate dielectrics on dc, radio frequency and linearity characteristics of lattice-matched AlInN/AlN/GaN metal–oxide–semiconductor high electron mobility transistor," IET Circuits Devices Syst. **10**, 423-432 (2016). https://doi.org/10.1049/iet-cds.2015.0332

[17] S. Baskaran, A. Mohanbabu, N. Anbuselvan, N. Mohankumar, D. Godwinraj, and C.K. Sarkar, "Modeling of 2DEG sheet carrier density and DC characteristics in spacer based AlGaN/AlN/GaN HEMT devices," Superlattices Microstruct. **64**, 470–482 (2013). http://dx.doi.org/10.1016/j.spmi.2013.10.019
[18] P. Dwivedi, and A. Kranti, "Applicability of transconductance-to-current ratio (g_m/I_{ds}) as a sensing metric for tunnel FET biosensors," IEEE Sensors J. **17**, 1030–1036 (2017). https://doi.org/10.1109/JSEN.2016.2640192
[19] A. Varghese, C. Periasamy, and L. Bhargava, "Analytical modeling and simulation-based investigation of AlGaN/AlN/GaN bio-HEMT sensor for C-erbB-2 detection," IEEE Sens. J. **18**, 9595–9602 (2018). https://doi.org/10.1109/JSEN.2018.2871718
[20] Y.F. Wu, S. Keller, P. Kozodoy, B.P. Keller, P. Parikh, D. Kapolnek, S.P. Denbaars, and U.K. Mishra, "Bias dependent microwave performance of AlGaN/GaN MODFET's up to 100 V," IEEE Electron. Dev. Lett. **18**, 290–292 (1997). https://doi.org/10.1109/55.585362
[21] W.D. Hu, X.S. Chen, Z.J. Quan, X.M. Zhang, Y. Huang, C.S. Xia, W. Lu, and P.D. Ye, "Simulation and optimization of GaN-based metal-oxide-semiconductor high electromobility-transistor using field-dependent drift velocity model," J. Appl. Phys. **102**, 034502 (2007). http://dx.doi.org/10.1063/1.2764206
[22] O. Ambacher, J. Smart, J.R. Shealy, N.G. Weimann, K. Chu, M. Murphy, W.J. Schaff, *et al*., "Two-dimensional electron gases induced by spontaneous and piezoelectric polarization charges in N- and Ga-face AlGaN/GaN heterostructures," J. Appl. Phys. **85**, 3222–3233 (1999). https://doi.org/10.1063/1.369664
[23] A.M. Bhat, A. Varghese, N. Shafi, and C. Periasamy, "A Dielectrically modulated GaN/AlN/AlGaN MOSHEMT with a nanogap embedded cavity for biosensing applications," IETE J. Res. **69**(3), 1419-1428 (2023). https://doi.org/10.1080/03772063.2020.1869593
[24] Y. Liu, X. He, Y. Dong, S. Fu, Y. Liu, and D. Chen, "The sensing mechanism of InAlN/GaN HEMT," Cryst. **12**, 401 (2022). https://doi.org/10.3390/cryst12030401

ПОРІВНЯЛЬНЕ ДОСЛІДЖЕННЯ ТА АНАЛІТИЧНЕ МОДЕЛЮВАННЯ БІОСЕНСОРОВ НА ОСНОВІ AlGaN/GaN HEMT ТА MOSHEMT ДЛЯ ВИЯВЛЕННЯ БІОМОЛЕКУЛ

Абделла Бугенна[a], Абдельхаді Феддаг[b], Дріс Бугенна[c,d], Ібрагім Фарук Бугенна[e]

[a]Електротехнічна лабораторія Орана, Відділ електроніки, Факультет електротехніки, Науково-технічний університет Орана (MB-USTO), 31000, Оран, Алжир

[b]Кафедра електроніки. Факультет електротехніки Університет наук і технологій Орана, Лабораторія мікросистем і вбудованих систем, Оран, Алжир

[c]Лабораторія геоматики, екології та навколишнього середовища, факультет природознавства та життя, Університет Мустафи Стамбулі, Маскара, 29000, Туш, Алжир

[d]Common Core Science and Technology Department, Science and Technology Faculty, Mustapha Stambouli University of Mascara, 29000, Mascara, Algeria

[e]Кафедра електротехніки, Факультет науки та технологій, Університет Мустафи Стамбулі в Маскара, Маскара 29000, Алжир

У цьому дослідженні була розроблена модель для аналізу біосенсорів на основі високоелектронних транзисторів AlGaN/GaN (HEMT) і металооксидних напівпровідникових високоелектронних транзисторів (MOSHEMT). Модель фокусується на виявленні біомолекул, таких як ChOx, протеїн, стрептавідин і уриказа, шляхом модуляції діелектричної проникності. Параметри чутливості, що використовуються для виявлення біомолекул, включають струм стоку, транспровідність і чутливість стоку. Діелектрична проникність регулюється на основі конкретної біомолекули, яку відчуває біосенсор. Зміна діелектрика призводить до змін струму витоку зі збільшенням або зменшенням залежно від позитивного заряду біомолекул. Пристрій HEMT демонструє більші варіації струму стоку, транспровідності та чутливості стоку порівняно з пристроєм MOSHEMT, коли біомолекула присутня в області порожнини. Результати моделювання підтверджуються шляхом їх порівняння з Atlas-TCAD (система автоматизованого проектування атласної технології) та експериментальними даними, що демонструє чудову згоду.

Ключові слова: *AlGaN/GaN; HEMT; MOSHEMT; біосенсори; біомолекули*